Evolutionary and biochemical analyses reveal conservation of the Brassicaceae telomerase ribonucleoprotein complex

Kelly Dew-Budd[2], Julie Cheung[2], Anna Nelson-Dittrich, Kyle Palos, Evan S. Forsythe, Andrew D. L. Nelson and Mark A. Beilstein[1]

School of Plant Sciences, University of Arizona, Tucson, Arizona 85721

[1]Corresponding Author: Mark A. Beilstein

School of Plant Sciences
University of Arizona
Tucson, Arizona 85721
mbeilstein@email.arizona.edu

[2]These authors contributed equally

Abstract:

The telomerase ribonucleoprotein complex (RNP) is essential for genome stability and performs this role through the addition of repetitive DNA to the ends of chromosomes. The telomerase enzyme is composed of a reverse transcriptase (TERT), which utilizes a template domain in an RNA subunit (TER) to reiteratively add telomeric DNA at the ends of chromosomes. Multiple TERs have been identified in the model plant *Arabidopsis thaliana.* Here we combine a phylogenetic and biochemical approach to understand how the telomerase RNP has evolved in Brassicaceae, the family that includes *A. thaliana*. Because of the complex phylogenetic pattern of template domain loss and alteration at the previously characterized *A. thaliana* TER loci, *TER1* and *TER2*, across the plant family Brassicaceae, we bred double mutants from plants with a template deletion at *AtTER1* and T-DNA insertion at *AtTER2*. These double mutants exhibited no telomere length deficiency, a definitive indication that neither of these loci encode a functional telomerase RNA. Moreover, we determined that the telomerase components *TERT*, *Dyskerin*, and the *KU* heterodimer are under strong purifying selection, consistent with the idea that the TER with which they interact is also conserved. To test this hypothesis further, we analyzed the substrate specificity of telomerase from species across Brassicaceae and determined that telomerase from close relatives bind and extend substrates in a similar manner, supporting the idea that TERs in different species are highly similar to one another and are likely encoded from an orthologous locus. Lastly, TERT proteins from across Brassicaceae were able to complement loss of function *tert* mutants *in vivo*, indicating TERTs from other species have the ability to recognize the native TER of *A. thaliana*. Finally, we immunoprecipitated the telomerase complex and identified associated RNAs via RNA-seq. Using our evolutionary data we constrained our analyses to conserved RNAs within Brassicaceae that contained a template domain. These analyses revealed a highly expressed locus whose disruption by a T-DNA

47 resulted in a telomeric phenotype similar to the loss of other telomerase core proteins, indicating
48 that the RNA has an important function in telomere maintenance.

49 **Introduction**

50 Chromosomes in most eukaryotes are capped by tandem TG-rich DNA repeats called
51 telomeres. The telomere repeat is remarkably conserved across deep evolutionary divergences.
52 For example, the repeat sequence TTTAGGG present in the majority of examined plants differs
53 by a single nucleotide from the vertebrate repeat TTAGGG [1]. Telomeric DNA repeats are
54 recognized and bound by a suite of proteins that are essential for chromosome end protection
55 and telomere replication [2], while telomere length is maintained by a ribonucleoprotein (RNP)
56 complex, which minimally consists of a telomerase reverse transcriptase (TERT) and a
57 telomerase RNA (TER). A template region within TER is complementary to approximately 1.5x
58 the telomere repeat and is used by TERT to synthesize telomeric DNA at the chromosome
59 terminus [3]. Although TERT and TER are sufficient to catalyze telomerase activity *in vitro*, *in*
60 *vivo* TER serves as a scaffold for the assembly of essential accessory proteins that have a
61 variety of functions including RNP biogenesis and recruitment of the RNP to the chromosome
62 end [4]. Many of these accessory proteins do not interact directly, but only associate with one
63 another via their interactions with TER [5,6]. Thus, TER is essential both as a template for
64 telomere synthesis, and as a core scaffolding molecule in telomerase assembly.

65 TERT proteins from distantly related species across the eukaryotic tree are readily
66 identifiable by homology searches based on amino acid sequence [3]. Given the essential role
67 of TER in telomere repeat addition and binding accessory proteins, a logical expectation would
68 be that TER would also display high levels of sequence conservation. However, TERs from
69 different eukaryotic lineages are highly variable at the nucleotide level and appear to be entirely
70 non-homologous, and thus independently evolved in each of the major eukaryotic lineages (i.e.,

animals, ciliates, fungi, and plants) [7,8]. Interestingly, most described TERs have converged on similar structural features that likely result from the shared requirement to bind both TERT and telomerase accessory proteins [6]. Two such core TER features include a pseudoknot, which is necessary for activity, and a stem loop domain (termed CR4/CR5, stem loop IV, and three way junction (TWJ) in vertebrates, ciliates, ascomycetes, respectively), which is necessary for TERT binding [9–12].

Bioinformatics approaches to recover TER have limits across major lineages of the eukaryotic crown group, but within eukaryotic clades TERs have been successfully recovered using a variety of sequence similarity based approaches. For example, in vertebrates Chen et al. (2000) recovered TER from species across the ~450 million year radiation using sequence similarity searches and positional conservation (synteny) to identify eight conserved domains [10]. Similarly, budding yeast and its closest relatives in *Saccharomyces sensu stricto*, a radiation spanning ~20 million years of evolution, encode TER at a syntenic locus, a fact that permitted bioinformatic detection of structurally conserved domains through signatures of covariation [13]. In the Pezizomycotina (Ascomycota), with the exception of *Saccharomyces s.s.*, TERs display sufficient conservation to facilitate identification by BLAST using the *Neurospora crassa TER* as query. Similarly, using a combination of template sequence identification and structural motif modeling from Pezizomycotina TERs, Qi et al. (2013) recovered TERs from the more distantly related Taphrinomycotina [12]. Thus, while biochemical approaches have been required to identify TER in each major crown group lineage of eukaryotes, bioinformatics approaches have aided discovery of TER within lineages.

Until recently, the only known functional TER in plants was from *Arabidopsis thaliana*. Cifuentes-Rojas et al. (2011) found that *A. thaliana* was unusual among studied eukaryotes because it encoded two TERs: *TER1* and *TER2* [14]. *TER1* was hypothesized to serve the canonical function in providing a template for telomere addition by telomerase *in vivo*. *TER2* has

96 the same template domain as *TER1*, but it is encoded at a different locus and has been
97 hypothesized to have an alternative function in regulating telomerase activity during genome
98 stress caused in part by double strand DNA breaks [15,16]. Both *AtTER1* and *AtTER2* were
99 shown to assemble *in vivo* into a telomerase RNP that includes *TERT*, although the accessory
100 proteins with which they assemble differ [14]. Importantly, the *TER2* RNP has not been
101 observed to contribute to telomere length maintenance.

102 Attempts to use bioinformatics approaches to identify the TER-encoding locus or loci
103 similar to *AtTER1* or *AtTER2* from other Brassicaceae have yielded surprising results. For
104 example, in 15 sampled species of the family, spanning 60 million years of evolution [17], there
105 is a single locus with sequence similarity to both *AtTER1* and *AtTER2* [18]. Sequence alignment
106 of the recovered *AtTER1/2-like* loci from the 15 sampled species revealed changes at the
107 template domain in four and the complete absence of a template-like domain in three. In order
108 for the four loci with template mutations to encode for TER, a corresponding change in the
109 telomere repeat should be observed [18]. However, genomic data from several of these
110 species, including *Arabidopsis lyrata* and *Capsella rubella*, indicate the plant telomere repeat is
111 conserved [19], suggesting the presence of an alternative TER locus. Although TER is known to
112 evolve rapidly at the sequence level in other systems, the rapid rate of novel TER incorporation
113 suggested by the identification of *AtTER1* is unprecedented. Recently, Fajkus et al. (2019)
114 showed that *AtTER1* mutants do not exhibit telomere shortening, and thus does not act as a
115 bona fide telomerase RNA [20].

116 Here we generate double mutants at *AtTER1* and *AtTER2* and verify that *AtTER2* does
117 not play a compensatory role in telomere length maintenance in the absence of *AtTER1*. Due to
118 the previously documented rapid evolution at the *AtTER1/2-like* locus [18], we sought to
119 determine the evolutionary conservation of the telomerase complex using a series of
120 comparative evolutionary and biochemical analyses on the protein constituents of telomerase.

121 Interestingly, rather than concluding that TER and components of telomerase are evolving
122 rapidly as the evolutionary history of *AtTER1/2* suggested, we find that the protein components
123 of telomerase are highly conserved, as is the biochemical activity of telomerase. We performed
124 an RNA immunoprecipitation using core protein components of the telomerase holoenzyme,
125 followed by RNA-sequencing, and then used our evolutionary data to constrain possible
126 template-bearing TER candidates to those that were conserved across the Brassicaceae family.
127 This alternative approach led to the identification of the conserved plant TER discovered by
128 Fajkus et al. (2019). Our data indicate that telomerase core components are highly conserved
129 and our data complements the findings in Fajkus et al. (2019) in verifying that the biochemical
130 activity of the holoenzyme is also conserved. Finally, we explore the possibility that the
131 previously documented *AtTER-like* locus in Brassicaceae shares the *AtTER2* function of
132 modulating telomerase activity during genotoxic stress.

133 **Results and Discussion**

134 **Double *AtTER1/AtTER2* mutants lack a telomere phenotype.** Beilstein et al. (2012) showed
135 that the *TER1/2-like* locus was not conserved throughout the Brassicaceae family, or even in
136 other species of the genus *Arabidopsis*. This led us to re-examine the conservation of *AtTER1*
137 among the ecotypes of *A. thaliana*. Using genomic data from 1001genomes.org, we generated
138 an alignment of the *AtTER1* locus using MEGA5 and sorted through the template domain in
139 Geneious (Biomatters, Inc.) [21,22]. We found that *AtTER1* had a mutated template domain in
140 41/853 *A. thaliana* ecotypes (TCCCAAA**T** -> TCCCAAA**A**), which would preclude the use of an
141 *AtTER1* transcript for telomere elongation in these ecotypes. Until the recently published work of
142 Fajkus et al. (2019), previous characterization of the *AtTER1* phenotype was performed using
143 an RNAi knock-down approach [14]; therefore, we generated a template deletion mutant at
144 *AtTER1*.

145 A telomerase RNA cannot perform its templating function without an intact template
146 domain, and thus we independently used CRISPR-Cas9 nuclease and CRISPR-Cas9-D10
147 nickase to create full template deletions at the *AtTER1* locus. We recovered two alleles that
148 lacked the template domain in its entirety (Fig 1A), *Atter1 Δ18* and *Atter1 Δ22*. First generation
149 homozygous mutants showed no reduction in telomere length as measured by telomere
150 restriction fragment length analysis (TRF) (Fig 1B). We then propagated both *ter1* homozygous
151 template nulls for several generations and measured telomere length in order to determine
152 whether there was progressive loss over time. We observed no reduction in telomere length for
153 either template-null mutant allele, regardless of generation (Fig 1B). Thus, our data definitively
154 indicate that *AtTER1* alone does not function as the template for telomere elongation,
155 confirming the findings in Fajkus et al. 2019.

156 **Fig 1. Double knockout of *TER1* and *TER2* does not decrease telomere length.** (A) Two
157 *Atter1* mutants were created using either CRISPR-Cas9 nuclease or nickase. The complete
158 deletion of the template domain precludes the use of *AtTER1* as the template for telomere
159 extension. (B) TRF analyses were performed on individual plants with two biological replicates
160 in a population segregating the indicated *ter1* allele (Δ18 or Δ22), and in successive generations
161 (G4 and G5). (C) TRF analyses were performed on two sets of double mutant (*ter1 Δ22/ter2-2*
162 and *ter1 Δ18/ter2-3*) populations segregating the indicated mutations. A '+' indicates a
163 homozygous wild type individual for the indicated gene and a '-' represents a homozygous
164 mutant for the indicated gene.

165 To rule out the possibility that *AtTER2* acts in a compensatory role to elongate telomeres
166 in the absence of *AtTER1*, we crossed both *Atter1* template null alleles (*Atter1 Δ18* and *Atter1*
167 *Δ22*), with two *Atter2* T-DNA mutants (*Atter2-2* and *Atter2-3*), to create homozygous double
168 mutants and then measured telomere length by TRF. Neither single mutants for either gene, nor
169 double mutants showed a decrease in telomere length (Fig 1C). Taken together, the lack of

170 decrease in telomere length in both the single and double mutants indicates that *A. thaliana*
171 requires neither the *AtTER1* nor the *AtTER2* locus to elongate telomeres.

172 **Telomerase RNP evolution is under purifying selection in Brassicaceae.** Relatively high
173 levels of conservation of the telomerase RNA within major eukaryotic lineages has allowed for
174 the identification of distantly related TERs within those lineages. It was the unprecedented lack
175 of conservation of the template domain at *AtTER1* within *A. thaliana* and *AtTER1/2-like* locus
176 within other species of Brassicaceae that motivated further exploration of telomerase RNP
177 evolution and function. Numerous genome expansions and contractions within the Brassicaceae
178 family [23] have created opportunities for gene neofunctionalization or subfunctionalization,
179 potentially leading to incorporation of novel subunits into the telomerase RNP in Brassicaceae,
180 including the potential for alternative TERs [18]. If novel subunits have been incorporated into
181 the telomerase RNP, we might expect the core subunits to undergo structural or chemical
182 changes associated with the accommodation of novel binding partners. These changes would
183 be expected to arise under positive selection. Alternatively, if the telomerase RNP has not
184 undergone this type of change, we would expect the core subunits to evolve under purifying
185 selection. With this in mind, we sought to determine if major protein components of the
186 telomerase RNP exhibited signatures of positive selection, indicating underlying changes to the
187 complex, or purifying selection, indicating a stable RNP. We tested for positive selection in
188 *TERT* along several branches within the Brassicaceae. In total, we tested five branches
189 indicated by roman numerals in Figure 2 using the branch-sites test in PAML 4.4b [24]. In each
190 case we recovered no evidence that *TERT* evolved under elevated rates of non-synonymous to
191 synonymous substitutions (Fig 2), suggesting that *TERT* remains under strong purifying
192 selection.

193 **Fig 2. Tests for signatures of positive selection in TERT evolution in Brassicaceae.**
194 Branches throughout the Brassicaceae phylogeny, indicated by italicized roman numerals and

195 bolded branches, were tested for positive selection, Likelihood ratio tests were performed on the
196 bolded branches using PAML (codeml) to compare the likelihood scores of models of evolution
197 that either include site classes with ω values ≥ 1 (Alt = Alternative model) or explicitly exclude
198 these site classes (Null = Null model). Alternative model likelihood scores that are ≥ 1.92 better
199 than null model likelihood scores indicate a significant signal of positive selection ($p<0.05$) along
200 the specified branch (denoted as *i-vi* on the tree).

201 In addition to *TERT*, we also searched for evidence of positive selection in three other
202 genes that encode telomerase accessory factors in *A. thaliana*. Dyskerin is a pseudouridine
203 synthase necessary for maturation of rRNA that has also been shown to be an essential
204 component of telomerase in *A. thaliana* and many other eukaryotes [25]. KU is a heterodimer
205 composed of KU70 and KU80 that associates with telomerase in humans, budding yeast, and
206 *A. thaliana* via Ku80-telomerase interactions [15,26,27]. KU plays dual roles as a key factor in
207 double-strand DNA break repair via the non-homologous end-joining pathway, as well as
208 telomere maintenance [28,29]. With the exception of the branches leading to *C. rubella* (iii) and
209 *S. irio/B. rapa* (vi) for *DYSKERIN* and *A. lyrata KU70*, we found no evidence of positive selection
210 (S1 Figure). Thus, contrary to our initial expectations, the protein components of telomerase are
211 not responding at the molecular level to genome duplications or contractions, such as those that
212 occurred in species like *B. rapa*. These findings support the idea that a highly conserved TER
213 locus may be present and functional in Brassicaceae.

214 **An evolutionary analysis of Brassicaceae telomerase enzymology recapitulates the**
215 **accepted organismal phylogeny.** We next sought to take an indirect, but more fine-scale
216 evolutionary look at how conserved TERs are in Brassicaceae, specifically in the region within
217 and adjacent to the template domain. The ability of telomerase to bind and extend a substrate
218 comes from TERT-substrate and TER-substrate interactions [8]. In addition, telomere synthesis
219 requires Watson-Crick base-pairing between the 3' end of the DNA substrate and the beginning

220 of the template domain within TER [30]. Thus, changes within and surrounding the template
221 domain can lead to differential alignment on a telomere substrate or premature product
222 dissociation, particularly when these changes occur within the 3' end of the template region [31–
223 33]. With this rationale in mind, we set out to determine if the origin of the structurally similar
224 Brassicaceae TERs came from one evolutionary event (i.e., an alternative TER locus with
225 shared ancestry for all Brassicaceae) or multiple independent evolutionary events (i.e.,
226 alternative TER loci in each species that converged rapidly on a similar TER structure).

227 To distinguish between these two possibilities, telomerase substrate utilization was
228 performed in ten species across Brassicaceae (Fig 3; S2 Figure). To generate a profile of
229 substrate utilization, we used the telomere repeat amplification protocol (TRAP) on partially
230 purified plant extracts incubated with a suite of oligos of different lengths and 3' end
231 composition, ranging from one to three nucleotides capable of Watson-Crick base-pairing with a
232 TER template (Fig 3; S2 Figure) [34]. Radio-labeled products were separated on a
233 polyacrylamide sequencing gel and compared against an oligo expected to produce the shortest
234 telomere permutation based on previous observations (N_{15}-GGG; Fig 3) [35]. Observed
235 differences in size between products relative to this oligo were measured and recorded as a
236 value of 0-6 using *A. thaliana* as the baseline (Fig 3, S2A Figure). A substrate utilization profile
237 was then generated for nine other species within Brassicaceae, including several close relatives
238 to *A. thaliana* (three biological replicates per species; summarized in Fig 3; S2B Figure). This
239 profile was then compared against the phylogenetic tree reflecting the known relationships
240 among these species (Fig 3).

241 **Fig 3. Substrate utilization by Brassicaceae telomerase RNPs closely resembles the**
242 **organismal phylogeny.** Substrate utilization profile for telomerase RNPs across ten
243 Brassicaceae. Left, the accepted organismal phylogeny of species examined. Right, substrate
244 utilization profile for all tested species. Telomerase extracts were incubated with a suite of oligos

245 of varying length and nucleotide composition. The site of binding and number of nucleotides
246 added prior to the first full repeat dictate the size of products produced. The lengths of each
247 product were determined by comparing against the shortest permutation (N15-GGG). Observed
248 product differences relative to N15-GGG were calculated for all species and oligo combinations.
249 The intensity with which the numbered boxes are shaded corresponds to the degree to which
250 the results differ from A. thaliana.

251 The substrate utilization profiles we generated for Brassicaceae telomerase closely
252 recapitulated the evolutionary history of the family (Fig 3). The Arabidopsis clade, along with *C.*
253 *rubella*, all utilized the suite of oligos in the same manner (White boxes; Fig 3). Importantly, *A.*
254 *arabicum*, which represents the earliest diverging lineage in Brassicaceae [36], shares the
255 profile of *A. thaliana*, despite 55 million years of evolution. Thus, these data support a model for
256 shared ancestry of a TER locus in all Brassicaceae.

257 **Distantly related Brassicaceae TERTs assemble into a functional telomerase RNP in *A.***
258 ***thaliana*.** To confirm our evolutionary analyses indicating that both the protein and RNA
259 components of the telomerase RNP are likely highly conserved across Brassicaceae, we
260 attempted to complement *A. thaliana tert* null lines with the genomic version of *TERT* from four
261 species in the group: *Capsella rubella, Cardamine hirsuta, Eutrema salsugineum*, and
262 *Schrenkiella parvula* [37]. The ability to complement *A. thaliana tert* null mutants with TERTs
263 from divergent species would indicate high conservation of telomerase across Brassicaceae. In
264 *A. thaliana,* plants can survive for approximately nine generations in the absence of TERT [38].
265 During this time, telomeres progressively shorten until they reach a length sufficient to elicit a
266 DNA damage response that prohibits further cell division. We determined the degree to which
267 the *Attert* null was complemented by each of the transgenes using a chromosome arm-specific
268 telomere length assay known as PETRA [39,40]. In the wild type *A. thaliana* (Col-0)
269 background, telomeres for all three arms tested were between the typical 2-4 kilobase size

range (Figs 4A and 4C) [39]. As expected, telomeres in the unselected sixth generation *Attert* -/- mutants were between 0.5-2 kilobases in length (Figs 4A and 4C). The *AtTERT* transgene was able to complement the mutant background and restore telomeres back to wild type range (Figs 4A and 4C; three independent biological replicates for each construct). Telomeres in these lines were elongated further in the second generation, suggesting successful and complete complementation with this construct (Figs 4A and 4C). We observed similar or slightly better complementation with TERT from *S. parvula*, one of the most distantly related species in our study (Figs 4B and 4C) [17]. Interestingly, despite observing transcription of the *E. salsugineum, C. hirsuta*, and *C. rubella TERT* transgenes (S4 Figure), and telomerase activity in these complementation lines, we did not observe telomere elongation with these constructs (S3 Figure). However, with the exception of the 1L chromosome arm in *C. rubella*, there was no significant decrease in telomere length between the two generations we tested (S3B Figure), suggesting some degree of partial complementation.

Fig 4. *S. parvula* TERT complements loss of function *Attert* -/- mutants. (*A*) PETRA results of the unselected, untransformed (US) control, wild type *A. thaliana* (Col.), and *Attert* -/- mutants transformed with the *AtTERT* construct. Chromosome arms are depicted by 1L, 3L, and 5L and indicate the left arm of chromosomes 1, 3, and 5, respectively. T1 and T2 indicate the first and second generation after transformation. At least three independent T1 transformants were analyzed and then propagated to the second generation. (B) PETRA results of complementation of *Attert* -/- mutants by *S. parvula* (Sp) TERT. (C) Quantification of PETRA results from (A) and (B).

These data may represent an inability on the part of some of these *TERT*s to fully reconstitute telomerase in *A. thaliana*. However, *C. rubella, C. hirsuta,* and *E. salsugineum* all have short endogenous telomeres, ranging from 1-3 Kb [19]. *S. parvula*, in contrast, has telomeres closer in length to *A. thaliana*. Thus, what appears to be partial complementation in *A.*

295 *thaliana* may reflect some feature in the *C. rubella, C. hirsuta*, and *E. salsugineum* TERT protein
296 that governs the production of shorter telomeres. The observed complementation in *A. thaliana*
297 by TERTs from other Brassicaceae supports the hypothesis of a common TER secondary
298 structure in all Brassicaceae.

299 **Identification of an alternative telomerase RNA by immunoprecipitation of the telomerase**
300 **RNP followed by RNA-seq.** CRISPR induced template deletion mutants of both previously
301 described TER loci in *A. thaliana* indicated that neither is a bona fide TER. We performed a
302 series of immunoprecipitation (IP) experiments designed to purify the telomerase RNP from
303 floral tissue, seedling tissue, and plant cell culture, all of which express *TERT* at a high level
304 [37]. We tracked telomerase activity from our IP and input fractions using TRAP, and extracted
305 RNA from IP fractions with verified telomerase activity. Following cDNA synthesis we pooled
306 and sequenced the libraries from IP experiments that used either an anti-TERT or anti-POT1A
307 antibody. Sequencing yielded 164,505,451 total paired-end reads across the 20 IP experiments.
308 The resulting reads were mapped to the *A. thaliana* genome (TAIR 10) and long non-coding
309 RNAs (lncRNAs) were identified using Evolinc (Fig 5A) [41,42]. Interestingly, no reads mapped
310 to the *AtTER1* locus. We winnowed candidate TER loci by sorting through Evolinc predicted
311 lncRNAs to find those capable of generating the telomeric repeat and those that were
312 conserved across Brassicaceae, in accordance with our evolutionary analyses (Figs 2-4)
313 suggesting a highly conserved TER. From the candidate set, we identified five highly-expressed
314 loci exhibiting conservation across the family (Fig 5B). The locus with the highest average TPM
315 among those conserved in at least three of our representative Brassicaceae is the same locus
316 that was identified as a telomerase RNA, named *TR*, which was shown to be conserved across
317 land plants [20]. This locus was also previously identified as a lncRNA associated with hypoxic
318 stress, termed *AtR8*. Hereafter we will refer to this locus as *AtTR/R8* [43].

319 **Fig 5. Computational identification of a putative telomerase RNA.** (A) Flowchart showing
320 analysis pipeline for RNA-immunoprecipitation. (B) List of the five telomerase RNA candidates
321 identified through the analysis pipeline and ranked by highest average transcripts per million
322 (TPM). (C) TRF of *AtTR/R8* T-DNA insertion lines from wildtype through third generation (G3)
323 homozygous insertion lines with each lane representing separate individuals.

324 To confirm the involvement of this lncRNA in telomere maintenance, we obtained T-DNA
325 mutants of *AtTR/R8* and confirmed homozygosity. We grew these lines for three generations,
326 measuring telomere length using a TRF with each generation (Fig 5C). We found that
327 homozygous *Attr/r8* mutants showed discrete banding patterns similar to *Attert* mutants. This
328 phenotype is a hallmark of telomerase deficiency [38] and indicates an important role for
329 *AtTR/R8* in telomere maintenance.

330 **The *AtTER-like* locus is transcribed in other Brassicaceae.** The relatively high expression of
331 *AtTER2* and its reported role in the negative regulation of telomerase in *A. thaliana* [15] raises
332 the possibility that the transcript produced from the *AtTER1/2-like* locus may be acting as a
333 telomerase interacting RNA (TIR) similar to *AtTER2*. To address whether the *AtTER1/2-like* loci
334 recovered from other species of Brassicaceae could potentially encode a TIR, we tested
335 whether or not we could detect transcripts consistent with a TIR, but independent of the
336 transcription of the *RAD52-1A* mRNA. For our analyses we chose four species with varying
337 phylogenetic distances from *A. thaliana*: *C. rubella* (diverged ~20 MYA), *C. hirsuta* (diverged
338 ~35 MYA), *E. salsugineum* (diverged ~ 43 MYA), and *S. parvula* (diverged ~ 43 MYA) [17]. The
339 *AtTER1/2-like* locus partially overlaps *RAD52-1A* in each of these species, therefore we
340 performed RT-PCR on *RAD52-1A* in each species in order to map the intron-exon boundaries
341 (Fig 6A). Following cloning and sequencing of *RAD52-1A* mRNA, we designed reverse primers
342 that bind within the first intron of *RAD52-1A* and used it in combination with a forward primer in
343 the predicted 5' UTR (Fig. 6A and 6B). We amplified and sequenced transcripts from RT-PCR

344 products generated using this forward primer with a reverse primer in the first intron of *RAD52-*
345 *1A*. Our results indicate that either a lncRNA is produced at the locus in the tested species or
346 splice variants for *RAD52-1A* exist. Thus, whether the amplified RNAs are entirely distinct from
347 the transcript produced from *RAD52-1A* and if they are TIRs performing a similar role as
348 *AtTER2* remains an open question.

349 **Fig 6. The *AtTER1/2-like* locus is transcribed in four other Brassicaceae species.** (A)
350 Schematic of the *AtTER1/2-like* locus in the Brassicaceae species examined in this study. The
351 overlapping *RAD52-1A* locus is also shown. Known transcription start sites (or ones shown in
352 this study) are indicated by a solid arrow. Conserved but unverified TER transcription stop sites
353 are indicated by dashed vertical black lines. Exons are shown by dark grey boxes, while introns
354 are light grey. Primer binding sites for determining putative TER expression are shown as a
355 black arrow beneath each locus. Expected product length is shown. Exon/intron lengths and
356 positions are shown to scale. (B) Transcriptional analysis of the putative TER loci. RT-PCR was
357 performed to determine TER expression using primers designed in the 5' UTR and within the
358 second intron of *RAD52 1A* as shown in (A). RT-PCR was performed on *RAD52-1A* to
359 determine intron/exon boundaries.

360 **Conclusions**

361 Our results indicate that the original identification of the telomerase RNA in *A. thaliana* was
362 incorrect, in agreement with the findings of Fajkus et al. (2019). Moreover, our data indicate that
363 the true TER locus is highly conserved in the family, and that the telomerase holoenzyme
364 across the family shares both key protein components as well as biochemical activity.
365 Independently through RNA-seq of AtTERT and AtPOT1A pull downs, we identified *AtTR/R8*, a
366 highly conserved lncRNA within the Brassicaceae that has the potential to act as the canonical
367 TER. These results are further confirmed by recent work in Asparagaceae and a number of

368 other taxa [20]. Fajkus et al. (2019) indicated that the same locus is conserved in a variety of
369 species spanning land plant history, indicating a single evolutionary origin of plant TER. Our
370 work expands on the findings in Fajkus et al. (2019) by showing a direct interaction of this RNA
371 with the telomerase holoenzyme in multiple tissues and stages in development in *A. thaliana*.
372 Further, we showed that despite sequence changes to any potential telomerase RNAs, TERT
373 proteins from across the Brassicaceae family can at least partially rescue an *Attert* mutant. This
374 finding points to the evolutionary stability of the entire telomerase RNP complex. Finally,
375 whether *AtTER2* has a role as a telomerase regulatory RNA remains an open question. We
376 detected transcripts from the *AtTER1/2-like* locus in other Brassicaceae, but were unable to
377 verify if these represent splice variants of *RAD52A-1* or a distinct lncRNA product. One
378 important consideration is that the phenotypes observed for *AtTER2* under genomic stress may
379 be due to a partial protein product encoded from this locus in *A. thaliana*. Regardless, future
380 work on telomerase regulation is required to distinguish between these hypotheses.

381 **Materials and Methods**

382 **Plant Material and Propagation.** *A. thaliana* (Col-0) seed from Dr. Dorothy Shippen, Texas
383 A&M University; *C. rubella* from Dr. Steven Wright, University of Toronto; *C. hirsuta* seed from
384 Dr. Angela Hay, Max Planck Institute for Plant Breeding Research; *E. salsugineum* seed from
385 Dr. Karen Schumaker, University of Arizona; *S. parvula* seed from Drs. Maheshi Dassanayake
386 and Dong-Ha Oh, Louisiana State University were used in this research. Standard Arabidopsis
387 growth conditions were used for all species.

388 **CRISPR-Cas9 Mutation Analyses.** The suite of CRISPR plasmids from Schiml, et al. (2014)
389 were obtained from the Ohio State University Arabidopsis Biological Resources Center (ABRC)
390 and used for cloning of CRISPR-Cas9 and CRISPR-Cas9-D10A vectors, following the
391 procedure described in Schiml, et al. (2014) [44]. A protospacer (5'-

392 GGGTTTAGTTGTCGTCTGAT-3') overlapping the template domain of *AtTER1* was used in
393 conjunction with both Cas9 and Cas9-D10A; in addition, a second protospacer (5'-
394 TTGTCCGGCGACAGAAATGG-3') targeting 33 base pairs downstream of the template domain
395 was used with Cas9-D10A. T2's were screened using PCR of the *TER1* locus followed by
396 HindIII restriction digest for deletions of the entire template domain.

397 *Atter2* mutants *ter2-2* (SALK_121147) and *ter2-3* (SALK_140126) were obtained from
398 the ABRC then crossed to the two *ter1* alleles, *ter1 Δ22* and *ter1 Δ18*, respectively. The progeny
399 resulting from the crosses were hemizygous for a *ter2* allele and heterozygous for a *ter1* allele.
400 By selfing these individuals we obtained a population segregating the mutations for both genes
401 allowing direct comparisons between full siblings in TRF analyses.

402 **Nuclear Protein Isolation, TRAP, TRF and RT-PCR.** Nuclear extracts were obtained from
403 ~10g of seedling tissue as described elsewhere [14]. TRAP was performed as described
404 previously [25]. Briefly, 50ng of total protein, sourced from flower tissue, was added to a 25ul
405 final reaction volume containing ~3uC ^{32}P-dGTP, Gotaq hot start mastermix (Promega), and
406 400nM Forward TRAP primer. This mixture was placed at 37˚C for 45 minutes, followed by the
407 addition of 400nM TRAP Reverse primer. For a list of primers see Supplemental Table 1. PCR
408 followed with an initial 95˚C step for 3', followed by 95˚C for 15", 60˚C for 30", 72˚C for 1' 30"
409 and 35 cycles. TRAP products were resolved on a 6% acrylamide gel (19:1) with 7M urea. For
410 RNA extraction, SDS extraction buffer (final concentration of: 2mM Tris pH 7.5, 200uM EDTA
411 pH 8.0, 0.05% SDS) was added to 1ml of fraction supplemented with enough 3M sodium
412 acetate (300mM final concentration). Following vortexing, this mixture was phenol/chloroform
413 extracted and ethanol precipitated according to standard protocols. Terminal restriction
414 fragment (TRF) length analyses were performed as described in Nelson et al. (2014). In brief,
415 genomic DNA was extracted and digested with the restriction enzyme Tru1I, followed by a

416 Southern blot using the telomeric repeat as a probe. RT-PCR was performed as described
417 above using primers listed in Supplemental Table 1.

418 **Positive Selection Analyses.** We obtained CDS sequences for *TERT*, *Dyskerin*, *Ku70*, and
419 *Ku80* from 15 taxa (Brassicaceae or close relatives) from publicly available genomes using
420 CoGe, TAIR, Phytozome, and SALK [41,45,46]. *Branch-sites* likelihood ratio tests were
421 performed on the indicated branches of each gene tree using PAML (codeml) [24] to compare
422 the likelihood scores of models of evolution that either include site classes with ω values ≥ 1
423 (denoted Alt = Alternative model) or explicitly exclude these site classes (denoted Null = null
424 model). Alternative model Likelihood scores that are ≥ 1.92 better than null model Likelihood
425 scores indicate a significant signal of positive selection ($p < 0.05$) along the specified branch
426 (see critical values from chi-squared distribution table at one degree of freedom). For *Ku70* and
427 *Dyskerin*, *L. alabamica* was removed from our analysis because the inferred phylogeny was not
428 congruent with the accepted organismal phylogeny. The *C. hirsuta* branch was not tested for
429 *Ku70*/*80* and *Dyskerin*, as genomic sequence was not available for these genes.

430 **Substrate Specificity Analysis.** Substrate specificity was tested by replacing the TRAP
431 Forward G primer with alternative forward primers, keeping the reverse primer the same. These
432 products were resolved on a 6% acrylamide sequencing gel. The space between two bands
433 generated from the N15-GGG oligo was divided into seven quadrants (using ImageJ, NIH).
434 Where bands in other lanes migrate relative to these quadrants determines the value given to
435 them for "observed product difference."

436 ***tert* -/- Complementation.** Full length genomic *TERT* constructs were PCR amplified from each
437 species tested. These constructs were designed to include 2 Kb upstream and 0.5 Kb
438 downstream sequence to include appropriate regulatory regions. Constructs were cloned into
439 the promoter-less Gateway (Invitrogen) vector pH7WG using In-Fusion (Clontech) and then

440 sequence verified. *Agrobacterium tumefaciens* (strain GV3101) was used to transform this
441 binary vector into a fifth generation *tert* -/- *A. thaliana* background using the floral dip method
442 [47]. At least three independent transformed lines were identified for each construct. RT-PCR
443 was performed on each line to ensure transcription of the *TERT* transgene using primers
444 denoted in Supplemental Table 1. PETRA was performed as described in Heacock et al. (2004)
445 using subtelomeric primers specific for chromosome arms 1L, 3L, and 5L (see S1 Table for
446 primer sequence). Radioactive images were quantified using ImageJ (NIH).

447 **RNA Immunoprecipitation (RIP) of the Telomerase Complex and RNA-seq Library**
448 **Preparation:** 5.5-day old *A. thaliana* accession Columbia (Col-0) seedlings, 5-day old *A.*
449 *thaliana* T87 cell culture, and *A. thaliana* Col-0 flowers were used for IP experiments. Cell
450 culture was concentrated using Miracloth and the resulting powder was dried, packed, and
451 stored at -80 °C for IP. Samples were pulverized in liquid nitrogen and approximately 100 mg of
452 tissue powder was resuspended in 5 mL of cold RIP buffer (200 mM Tris-HCl pH 9, 110 mM
453 potassium acetate, 0.5 % Triton X-100, 0.1 % Tween 20, 2.5 mM dithiothreitol (DTT), 1.5 %
454 Protease Inhibitor Cocktail (Sigma-Aldrich P9599), 40 units/µL RNaseOUT (ThermoFisher
455 p10777019)) by pipetting. The 5 mL of homogenate was then centrifuged at 1,500 x g for 2
456 minutes at 4°C. From the resulting supernatant, 250 µL was kept as RIP input, and 5 µL was
457 kept for the TRAP assay.

458 Immunoprecipitation was performed by washing 150 µL of Protein A Dynabeads
459 (ThermoFisher, 10002D) twice with PBS (137 mM NaCl, 2.7 mM KCl, 10 mM sodium phosphate
460 dibasic, 2 mM sodium phosphate monobasic, pH 7.4) supplemented with 0.02% Tween 20.
461 Then, 5-10 µL of GFP (Abcam, ab290), TERT, or POT1A antibody was diluted to 600 µL with
462 PBS supplemented with 0.02 % *Tween* 20, 0.2 mg/mL Salmon Sperm DNA (ThermoFisher,
463 15632011), and 0.25 mg/mL BSA. Washed beads were resuspended in the antibody solution
464 and allowed to rotate at room temperature for 90 minutes.

465 After 90 minutes, the beads were separated from the antibody-PBS solution and
466 resuspended in 2 mL of the RIP extract. The bead-RIP mixture was rotated at 4°C for 3 hours.
467 After 3 hours, beads were washed 6 times with 1 mL cold RIP buffer and washed twice with 1
468 mL of cold TMG buffer (10 mM Tris-Acetate pH8, 1 mM $MgCl_2$, 1 mM DTT, 10 % glycerol).
469 Beads were resuspended in 150 µL of cold TMG buffer, 5 µL was kept for TRAP assay.

470 To purify the RNA associated with the telomerase RNA complex, we added 1 mL of
471 TRIzol Reagent (ThermoFisher, 15596026) to the 145 µL of remaining beads at the end of the
472 RIP experiment to extract RNA following manufacturer's instructions. RNA was treated with
473 TURBO DNase (ThermoFisher, AM2238) to degrade contaminating genomic DNA following the
474 manufacturer's instructions. RNA was purified from the DNase reaction by ethanol precipitation.
475 The RNA libraries were prepared using the YourSeq FT v1.5 kit (Amaryllis Nucleics) following
476 manufacturer's instructions. RNA samples checked for integrity using a Bioanalyzer throughout
477 preparation. RNA was sequenced using Illumina NextSeq 500 PE x 75bp.

478 **Computational Analysis of RNA-seq Data.** RNA purifications from POT1A and TERT
479 antibodies generated 164,505,451 total paired-end reads across 20 pull-down experiments.
480 Reads were mapped to the *A. thaliana* TAIR 10 reference genome using the Read Mapping and
481 Transcript Assembly workflow (RMTA v2.5.1.2) (github.com/Evolinc/RMTA) through the
482 CyVerse Discovery Environment (cyverse.org). RMTA utilizes Hisat2 [48] for read mapping, and
483 Stringtie [49] for transcript assembly as a seamless workflow. Default RMTA parameters were
484 used, besides specifying paired-end reads and changing the maximum intron length from
485 500,000 bp to 50,000. Read mapping for all experiments achieved at least 89% overall
486 alignment rates. Candidate loci were identified using Evolinc v1.7.5 [42]. Evolinc identifies and
487 annotates novel long intergenic noncoding RNAs (lincRNAs) using assembled transcripts from
488 RMTA as GTF files as well as information regarding surrounding annotated genes using a
489 reference genome annotation. Candidate lincRNAs from the 20 pull-down experiments were

490 merged with the reference genome annotation to a single annotation file using Evolinc merge for
491 subsequent analyses.

492 To quantify the expression of candidate loci, featureCounts v1.6.0 [50] was used
493 (specifying paired-end reads, feature types: exon, and gene attribute: gene_id) taking BAM files
494 from RMTA as input along with the merged annotation file. Gene expression was normalized
495 across the 20 pull-down experiments by converting counts to transcripts per million (TPM) which
496 accounts for feature length and sequencing depth.

497 To begin filtering for candidate telomerase RNAs, genes were only selected if they had
498 an average TPM (Transcripts per Kilobase Million) over 1 across the 20 experiments (78,487
499 features to 16,473 features). Candidates overlapping known genes, from TAIR 10, were then
500 discarded (16,473 features to 1,780 features). Candidate loci were then analyzed for putative
501 template domains by mapping all permutations of the telomere repeat "TTTAGGG" and its
502 reverse complement from 9 to 19 nt in length (154 possible permutations) to the 1,780
503 candidates using the software Geneious Prime 2019.2.1 (BioMatters, Inc.), resulting in 225
504 remaining candidate loci containing at least a 9 nt template domain.

505 Conservation analyses on the 225 candidate loci was performed using Evolinc-II which
506 identifies orthologous loci across a defined set of genomes, in this case from representative
507 species across the Brassicaceae family *(Arabidopsis thaliana, Arabidopsis lyrata, Capsella*
508 *rubella, Brassica oleracea, Brassica rapa, Eutrema salsugineum, Schrenkiella parvula,* and
509 *Aethionema arabicum*) as well as one species from the sister family, *Tarenaya hassleriana* in
510 Cleomaceae. Evolinc-II was used with an E-value cutoff of E-5 to allow for sequence divergent
511 orthologs to be identified. Finally, TER candidates were removed if a template containing
512 ortholog was not identified in at least 3 relatives, yielding 5 candidates.

513 **Telomere Length of AtTR/R8 T-DNA Lines.** The T-DNA line (FLAG-410H04) was obtained
514 from the Versailles INRA collection. Plants homozygous for the T-DNA were bred for three
515 generations to show the long term impact of a *AtTR/R8* loss on telomeres. The wildtype
516 comparison used for the TRF was a homozygous wildtype sibling obtained from a population
517 segregating for the FLAG-410H04 T-DNA insertion.

518 **Acknowledgements**

519 We thank Dr. Dorothy Shippen for the kind gift of anti-TERT and anti-POT1A antibodies, and
520 Jairui Song from the Shippen Lab for assistance with our immunoprecipitation experiments. In
521 addition, we thank the PaBeBaWoMo research group at the University of Arizona for insightful
522 and helpful comments during the completion of this project and members of the Beilstein lab for
523 help with plant cultivation, tissue collection, and moral support.

524

525 **References**

526 1. Watson JM, Riha K. Comparative biology of telomeres: Where plants stand. FEBS Lett.
527 2010;584: 3752–3759. doi:10.1016/j.febslet.2010.06.017
528 2. de Lange T. How Telomeres Solve the End-Protection Problem. Science (80-).
529 2009;326: 948–952. doi:10.1126/science.1170633
530 3. Autexier C, Lue NF. The Structure and Function of Telomerase Reverse Transcriptase.
531 Annu Rev Biochem. 2006;75: 493–517. doi:10.1146/
532 4. Egan ED, Collins K. Biogenesis of telomerase ribonucleoproteins. RNA. 2012;18: 1747–
533 1759. doi:10.1261/rna.034629.112
534 5. Collins K. The biogenesis and regulation of telomerase holoenzymes. Nat Rev Mol Cell
535 Biol. 2006;7: 484–494. doi:10.1038/nrm1961
536 6. Theimer CA, Feigon J. Structure and function of telomerase RNA. Curr Opin Struct Biol.

537 2006;16: 307–318. doi:10.1016/J.SBI.2006.05.005
538 7. Gunisova S, Elboher E, Nosek J, Gorkovoy V, Brown Y, Lucier J-F, et al. Identification
539 and comparative analysis of telomerase RNAs from Candida species reveal conservation
540 of functional elements. RNA. 2009;15: 546–59. doi:10.1261/rna.1194009
541 8. Blackburn EH, Collins K. Telomerase: an RNP enzyme synthesizes DNA. Cold Spring
542 Harb Perspect Biol. 2011;3. doi:10.1101/cshperspect.a003558
543 9. Lingner J, Hendrick LL, Cech TR. Telomerase RNAs of different ciliates have a common
544 secondary structure and a permuted template. Genes Dev. 1994;8: 1984–1998.
545 doi:10.1101/gad.8.16.1984
546 10. Chen J-L, Blasco MA, Greider CW. Secondary Structure of Vertebrate Telomerase RNA.
547 Cell. 2000;100: 503–514. doi:10.1016/S0092-8674(00)80687-X
548 11. Tzfati Y. A novel pseudoknot element is essential for the action of a yeast telomerase.
549 Genes Dev. 2003;17: 1779–1788. doi:10.1101/gad.1099403
550 12. Qi X, Li Y, Honda S, Hoffmann S, Marz M, Mosig A, et al. The common ancestral core of
551 vertebrate and fungal telomerase RNAs. Nucleic Acids Res. 2013;41: 450–462.
552 doi:10.1093/nar/gks980
553 13. Dandjinou AT, Lévesque N, Larose S, Lucier J-F, Elela SA, Wellinger RJ. A
554 Phylogenetically Based Secondary Structure for the Yeast Telomerase RNA. Curr Biol.
555 2004;14: 1148–1158. doi:10.1016/j.cub.2004.05.054
556 14. Cifuentes-Rojas C, Kannan K, Tseng L, Shippen DE. Two RNA subunits and POT1a are
557 components of Arabidopsis telomerase. Proc Natl Acad Sci U S A. 2011;108: 73–78.
558 doi:10.1073/pnas.1013021107
559 15. Cifuentes-Rojas C, Nelson ADL, Boltz KA, Kannan K, She X, Shippen DE. An alternative
560 telomerase RNA in Arabidopsis modulates enzyme activity in response to DNA damage.
561 Genes Dev. 2012;26: 2512–23. doi:10.1101/gad.202960.112
562 16. Xu H, Nelson ADL, Shippen DE. A Transposable Element within the Non-canonical

563 Telomerase RNA of Arabidopsis thaliana Modulates Telomerase in Response to DNA
564 Damage. Zhou J-Q, editor. PLOS Genet. 2015;11: e1005281.
565 doi:10.1371/journal.pgen.1005281
566 17. Beilstein MA, Nagalingum NS, Clements MD, Manchester SR, Mathews S. Dated
567 molecular phylogenies indicate a Miocene origin for Arabidopsis thaliana. Proc Natl Acad
568 Sci U S A. 2010;107: 18724–8. doi:10.1073/pnas.0909766107
569 18. Beilstein MA, Brinegar AE, Shippen DE. Evolution of the Arabidopsis telomerase RNA.
570 Front Genet. 2012;3: 1–8. doi:10.3389/fgene.2012.00188
571 19. Nelson ADL, Forsythe ES, Gan X, Tsiantis M, Beilstein MA. Extending the model of
572 Arabidopsis telomere length and composition across Brassicaceae. Chromosom Res.
573 2014;22: 153–166. doi:10.1007/s10577-014-9423-y
574 20. Fajkus P, Peška V, Závodník M, Fojtová M, Fulnečková J, Dobias Š, et al. Telomerase
575 RNAs in land plants. Nucleic Acids Res. 2019; doi:10.1093/nar/gkz695
576 21. Alonso-Blanco C, Andrade J, Becker C, Bemm F, Bergelson J, Borgwardt KM, et al.
577 1,135 Genomes Reveal the Global Pattern of Polymorphism in Arabidopsis thaliana. Cell.
578 2016;166: 481–491. doi:10.1016/j.cell.2016.05.063
579 22. Tamura K, Peterson D, Peterson N, Stecher G, Nei M, Kumar S. MEGA5: Molecular
580 Evolutionary Genetics Analysis Using Maximum Likelihood, Evolutionary Distance, and
581 Maximum Parsimony Methods. Mol Biol Evol. 2011;28: 2731–2739.
582 doi:10.1093/molbev/msr121
583 23. Bowers JE, Chapman BA, Rong J, Paterson AH. Unravelling angiosperm genome
584 evolution by phylogenetic analysis of chromosomal duplication events. Nature. 2003;422:
585 433–438. doi:10.1038/nature01521
586 24. Bielawski J, Yang Z. A Maximum Likelihood Method for Detecting Functional Divergence
587 at Individual Codon Sites, with Application to Gene Family Evolution. J Mol Evol. 2004;59:
588 121–132. doi:10.1007/s00239-004-2597-8

589 25. Kannan K, Nelson ADL, Shippen DE. Dyskerin Is a Component of the Arabidopsis
590 Telomerase RNP Required for Telomere Maintenance. Mol Cell Biol. 2008;28: 2332–
591 2341. doi:10.1128/MCB.01490-07
592 26. Stellwagen AE. Ku interacts with telomerase RNA to promote telomere addition at native
593 and broken chromosome ends. Genes Dev. 2003;17: 2384–2395.
594 doi:10.1101/gad.1125903
595 27. Ting NSY. Human Ku70/80 interacts directly with hTR, the RNA component of human
596 telomerase. Nucleic Acids Res. 2005;33: 2090–2098. doi:10.1093/nar/gki342
597 28. Jackson SP. Sensing and repairing DNA double-strand breaks. Carcinogenesis. 2002;23:
598 687–696. doi:10.1093/carcin/23.5.687
599 29. Bertuch AA, Lundblad V. The Ku Heterodimer Performs Separable Activities at Double-
600 Strand Breaks and Chromosome Termini. Mol Cell Biol. 2003;23: 8202–8215.
601 doi:10.1128/MCB.23.22.8202-8215.2003
602 30. Qi X, Xie M, Brown AF, Bley CJ, Podlevsky JD, Chen JJ-L. RNA/DNA hybrid binding
603 affinity determines telomerase template-translocation efficiency. EMBO J. 2012;31: 150–
604 161. doi:10.1038/emboj.2011.363
605 31. Gilley D, Blackburn EH. Specific RNA residue interactions required for enzymatic
606 functions of Tetrahymena telomerase. Mol Cell Biol. 1996;16: 66–75.
607 doi:10.1128/MCB.16.1.66
608 32. Wang H. A novel specificity for the primer-template pairing requirement in Tetrahymena
609 telomerase. EMBO J. 1998;17: 1152–1160. doi:10.1093/emboj/17.4.1152
610 33. Förstemann K, Lingner J. Telomerase limits the extent of base pairing between template
611 RNA and telomeric DNA. EMBO Rep. 2005;6: 361–366. doi:10.1038/sj.embor.7400374
612 34. Fitzgerald MS, McKnight TD, Shippen DE. Characterization and developmental patterns
613 of telomerase expression in plants. Proc Natl Acad Sci U S A. 1996;93: 14422–7.
614 doi:10.1073/pnas.93.25.14422

615 35. Fitzgerald MS, Shakirov E V., Hood EE, McKnight TD, Shippen DE. Different modes of
616 de novo telomere formation by plant telomerases. Plant J. 2001;26: 77–87.
617 doi:10.1046/j.1365-313x.2001.01010.x
618 36. Beilstein MA, Al-Shehbaz IA, Kellogg EA. Brassicaceae phylogeny and trichome
619 evolution. Am J Bot. 2006;93: 607–619. doi:10.3732/ajb.93.4.607
620 37. Fitzgerald MS, Riha K, Gao F, Ren S, McKnight TD, Shippen DE. Disruption of the
621 telomerase catalytic subunit gene from Arabidopsis inactivates telomerase and leads to a
622 slow loss of telomeric DNA. Proc Natl Acad Sci U S A. 1999;96: 14813–8.
623 doi:10.1073/pnas.96.26.14813
624 38. Riha K, McKnight TD, Griffing LR, Shippen DE. Living with genome instability: Plant
625 responses to telomere dysfunction. Science (80-). 2001;291: 1797–1800.
626 doi:10.1126/science.1057110
627 39. Heacock M, Spangler E, Riha K, Puizina J, Shippen DE. Molecular analysis of telomere
628 fusions in Arabidopsis: multiple pathways for chromosome end-joining. EMBO J. 2004;23:
629 2304–2313. doi:10.1038/sj.emboj.7600236
630 40. Heacock ML, Idol RA, Friesner JD, Britt AB, Shippen DE. Telomere dynamics and fusion
631 of critically shortened telomeres in plants lacking DNA ligase IV. Nucleic Acids Res.
632 2007;35: 6490–6500. doi:10.1093/nar/gkm472
633 41. Berardini TZ, Reiser L, Li D, Mezheritsky Y, Muller R, Strait E, et al. The arabidopsis
634 information resource: Making and mining the “gold standard” annotated reference plant
635 genome. genesis. 2015;53: 474–485. doi:10.1002/dvg.22877
636 42. Nelson ADL, Devisetty UK, Palos K, Haug-Baltzell AK, Lyons E, Beilstein MA. Evolinc: A
637 Tool for the Identification and Evolutionary Comparison of Long Intergenic Non-coding
638 RNAs. Front Genet. 2017;8: 52. doi:10.3389/fgene.2017.00052
639 43. Wu J, Okada T, Fukushima T, Tsudzuki T, Sugiura M, Yukawa Y. A novel hypoxic stress-
640 responsive long non-coding RNA transcribed by RNA polymerase III in Arabidopsis. RNA

641 Biol. 2012;9: 302–313. doi:10.4161/rna.19101
642 44. Schiml S, Fauser F, Puchta H. The CRISPR/Cas system can be used as nuclease for in
643 planta gene targeting and as paired nickases for directed mutagenesis in Arabidopsis
644 resulting in heritable progeny. Plant J. 2014;80: 1139–1150. doi:10.1111/tpj.12704
645 45. Lyons E, Pedersen B, Kane J, Alam M, Ming R, Tang H, et al. Finding and Comparing
646 Syntenic Regions among Arabidopsis and the Outgroups Papaya, Poplar, and Grape:
647 CoGe with Rosids. Plant Physiol. 2008;148: 1772–1781. doi:10.1104/pp.108.124867
648 46. Goodstein DM, Shu S, Howson R, Neupane R, Hayes RD, Fazo J, et al. Phytozome: a
649 comparative platform for green plant genomics. Nucleic Acids Res. 2012;40: D1178–
650 D1186. doi:10.1093/nar/gkr944
651 47. Zhang X, Henriques R, Lin S-S, Niu Q-W, Chua N-H. Agrobacterium-mediated
652 transformation of Arabidopsis thaliana using the floral dip method. Nat Protoc. 2006;1:
653 641–646. doi:10.1038/nprot.2006.97
654 48. Kim D, Langmead B, Salzberg SL. HISAT: a fast spliced aligner with low memory
655 requirements. Nat Methods. 2015;12: 357–360. doi:10.1038/nmeth.3317
656 49. Pertea M, Pertea GM, Antonescu CM, Chang T-C, Mendell JT, Salzberg SL. StringTie
657 enables improved reconstruction of a transcriptome from RNA-seq reads. Nat Biotechnol.
658 2015;33: 290–295. doi:10.1038/nbt.3122
659 50. Liao Y, Smyth GK, Shi W. featureCounts: an efficient general purpose program for
660 assigning sequence reads to genomic features. Bioinformatics. 2014;30: 923–930.
661 doi:10.1093/bioinformatics/btt656
662

663 **Figure Legends**

664 **Supplemental Fig 1. Positive selection analysis of Dyskerin, Ku70, and Ku80 in**
665 **Brassicaceae.** Roman numerals correspond to branches tested in Fig 2. Alternative model

666 likelihood scores that are significantly greater than null model likelihood scores indicate positive
667 selection ($p<0.05$) along the specified branch and are denoted in bold.

668 **Supplemental Fig 2. Substrate utilization of telomerase from different Brassicaceae**
669 **telomerase RNPs.** (*A*). Expected binding between AtTER1 template and each oligo used in the
670 experiment. The first set of nucleotides added by this template before the first full repeat is
671 shown in bold. Expected product differences are calculated relative to oligo #4, which is the
672 shortest oligo provided in the assay and therefore serves as the baseline. (*B*) A subset of the
673 gel image from the substrate utilization assay for each species tested. A dashed line is drawn
674 through the center of a band for oligo N15-GGG, which serves as the baseline for calculating
675 observed product differenced for the other oligos.

676 **Supplemental Fig 3. Test of complementation of *Attert* -/- background with genomic TERT**
677 **constructs from other Brassicaceae.** (*A*) PETRA results for Attert -/- lines transformed with *C.*
678 *rubella* TERT (Cr), *C. hirsuta* TERT (Ch), and *E. salsugineum* TERT (Es). (*B*) Quantification of
679 results shown in (*A*).

680 **Supplemental Fig 4. Confirmation of expression of TERT transgenes for**
681 **complementation experiments.** RNA was extracted from floral tissue from each background.
682 RT-PCR was performed on both the 3' end of the TERT transgene (shown) and the full-length
683 construct (not shown). GAPDH was used to determine quality of RNA and as an approximate
684 loading control. "+" indicates a positive RT reaction, whereas "-" indicates no reverse
685 transcriptase was added.

A

Allele	Sequence	CRISPR Type
	Template	
Wild type	TTTCGTGCCTATCAGACGACAACTAAACCCTACACGCTTACATA	
At*ter1 Δ18*	TTTCGTGCCTATCAG----------ACGCTTACATA	Cas9-D10A
At*ter1 Δ22*	TTTCGTGCCTATC----------GCTTACATA	Cas9

B

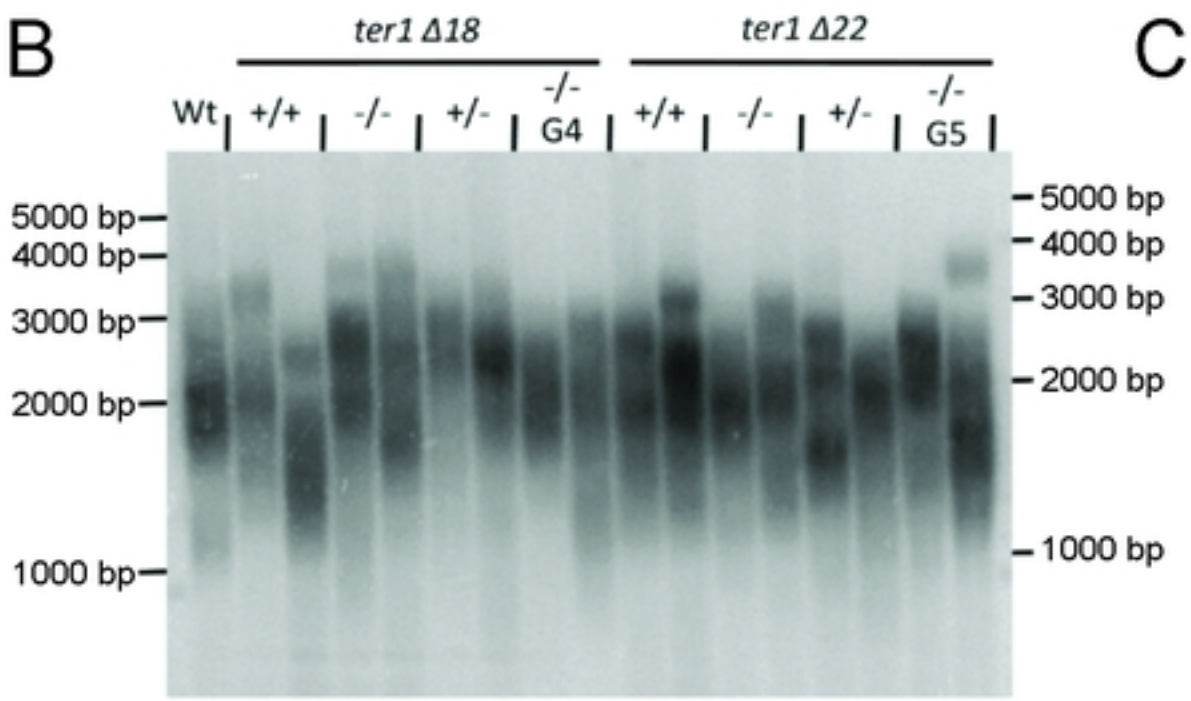

C

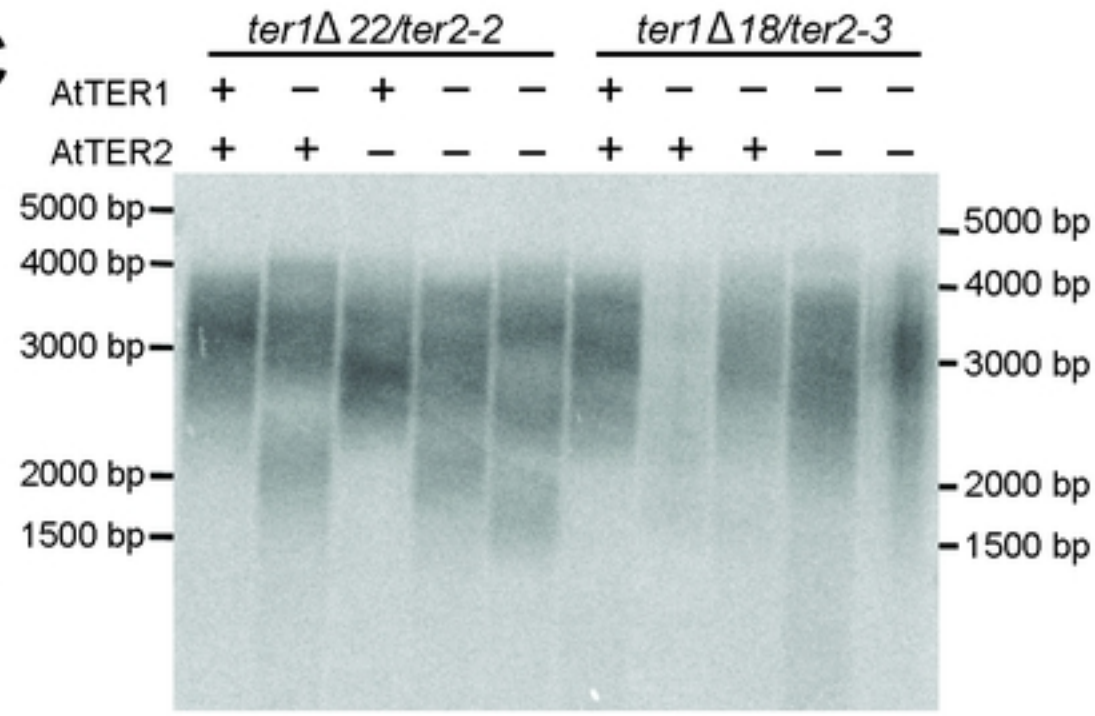

Figure 1

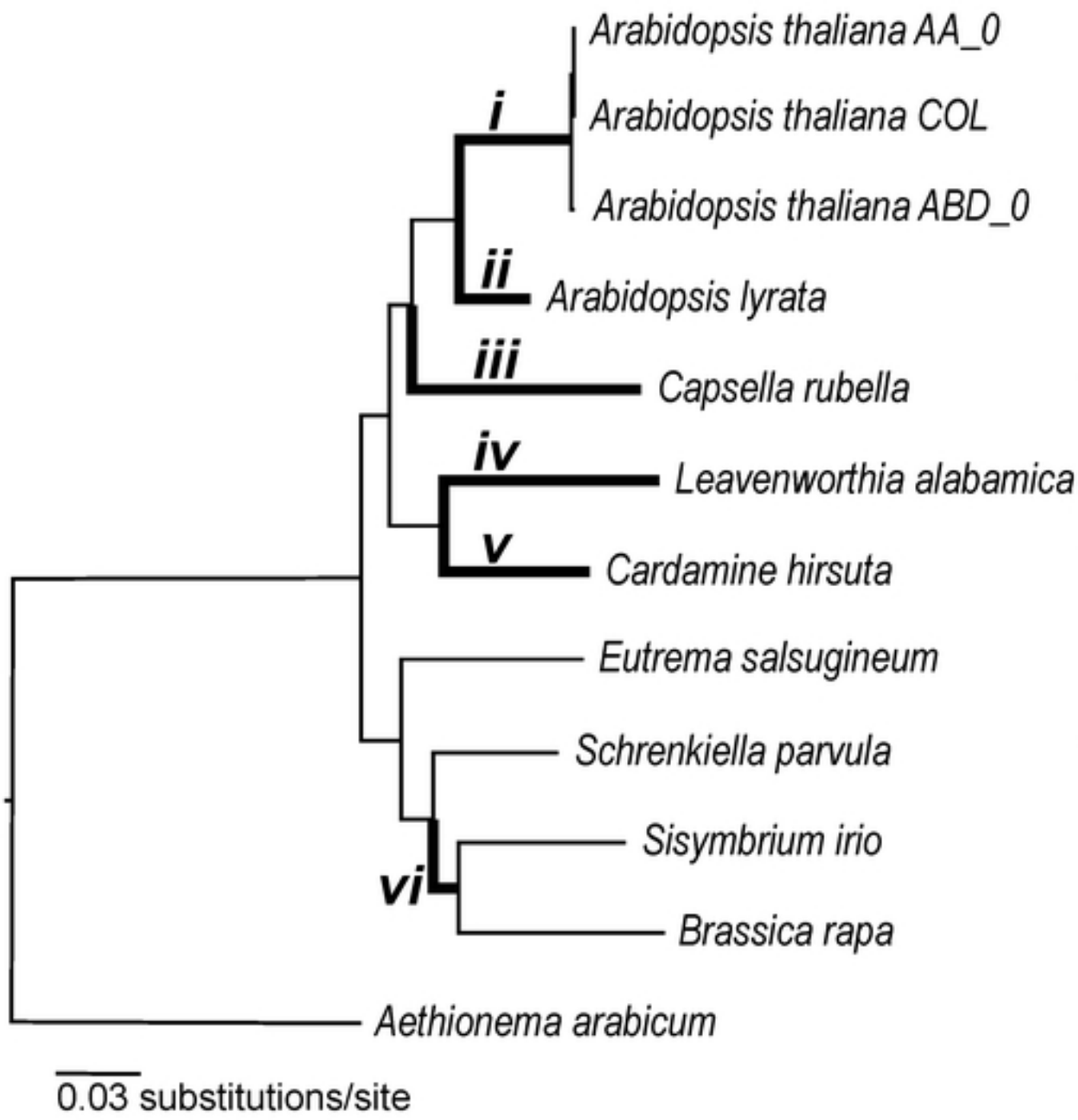

i	Null lnL = - 16053.566 (ω ≤ 1) Alt lnL = - 16051.716 (1 ≤ ω) p > 0.05 Not Significant
ii	Null lnL = - 15796.436 (ω ≤ 1) Alt lnL = - 15796.436 (1 ≤ ω) p > 0.05 Not Significant
iii	Null lnL = - 15797.307 (ω ≤ 1) Alt lnL = - 15797.307 (1 ≤ ω) p > 0.05 Not Significant
iv	Null lnL = - 15797.374 (ω ≤ 1) Alt lnL = - 15797.374 (1 ≤ ω) p > 0.05 Not Significant
v	Null lnL = - 15797.488 (ω ≤ 1) Alt lnL = - 15797.488 (1 ≤ ω) p > 0.05 Not Significant
vi	Null lnL = - 15797.589 (≤ 1) Alt lnL = 15797.581 (1 ≤ ω) p > 0.05 Not Significant

Figure 2

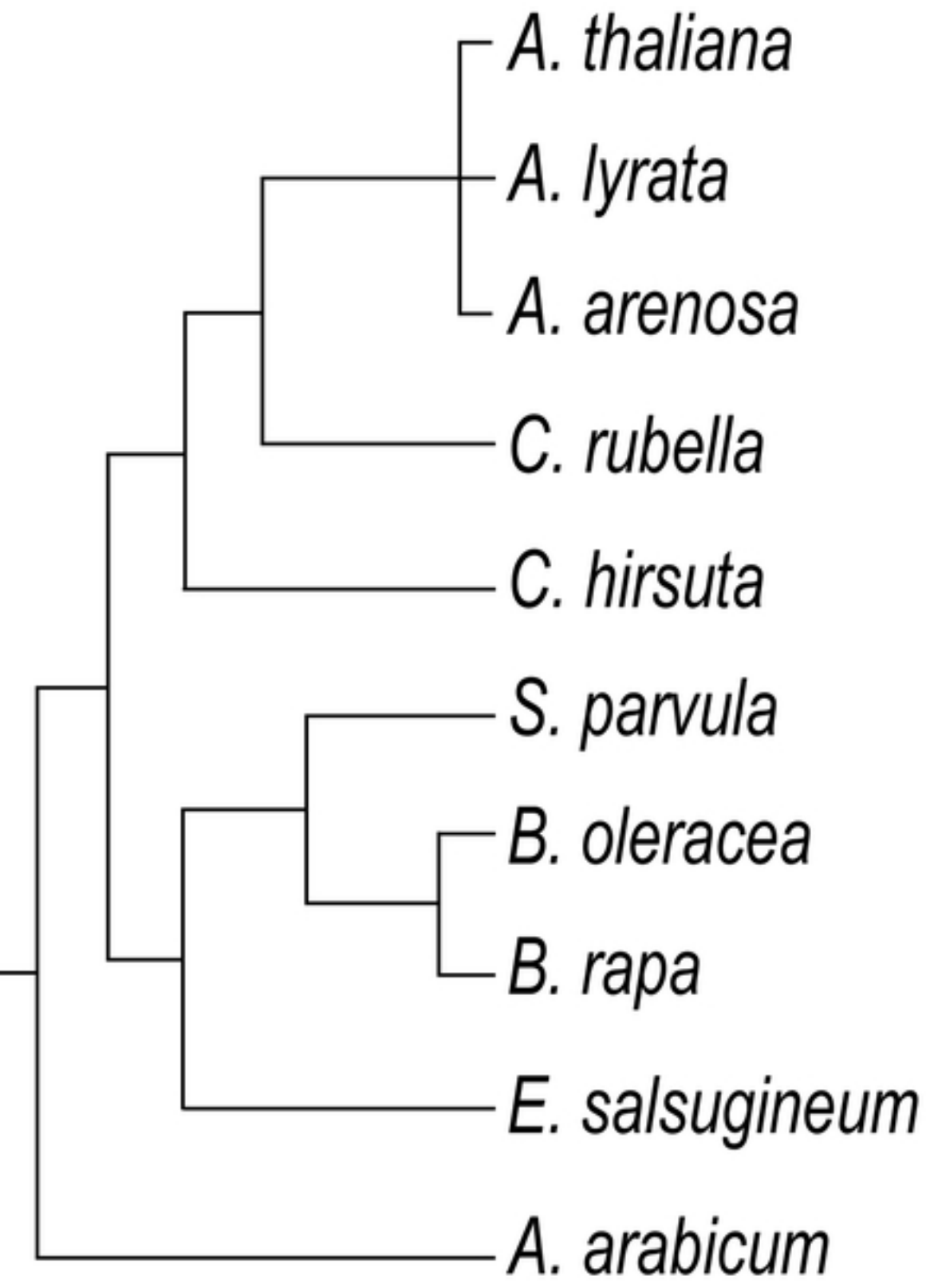

Observed Product Difference Relative to N15-GGG

Oligo used	N19-AG	N19-GG	N18-GGG	N15-GGG	N19-TT	N20-T	N17-T
A. thaliana	4	4	3	0	1	6	3
A. lyrata	4	4	3	0	1	6	3
A. arenosa	4	4	3	0	1	6	3
C. rubella	4	4	3	0	1	6	3
C. hirsuta	5	4	3	0	1	4	1
S. parvula	4	4	3	0	1	6	4
B. oleracea	3	3	2	0	1	4	2
B. rapa	3	3	2	0	1	4	2
E. salsugineum	4	4	3	0	1	4	2
A. arabicum	4	4	3	0	1	6	3

Figure 3

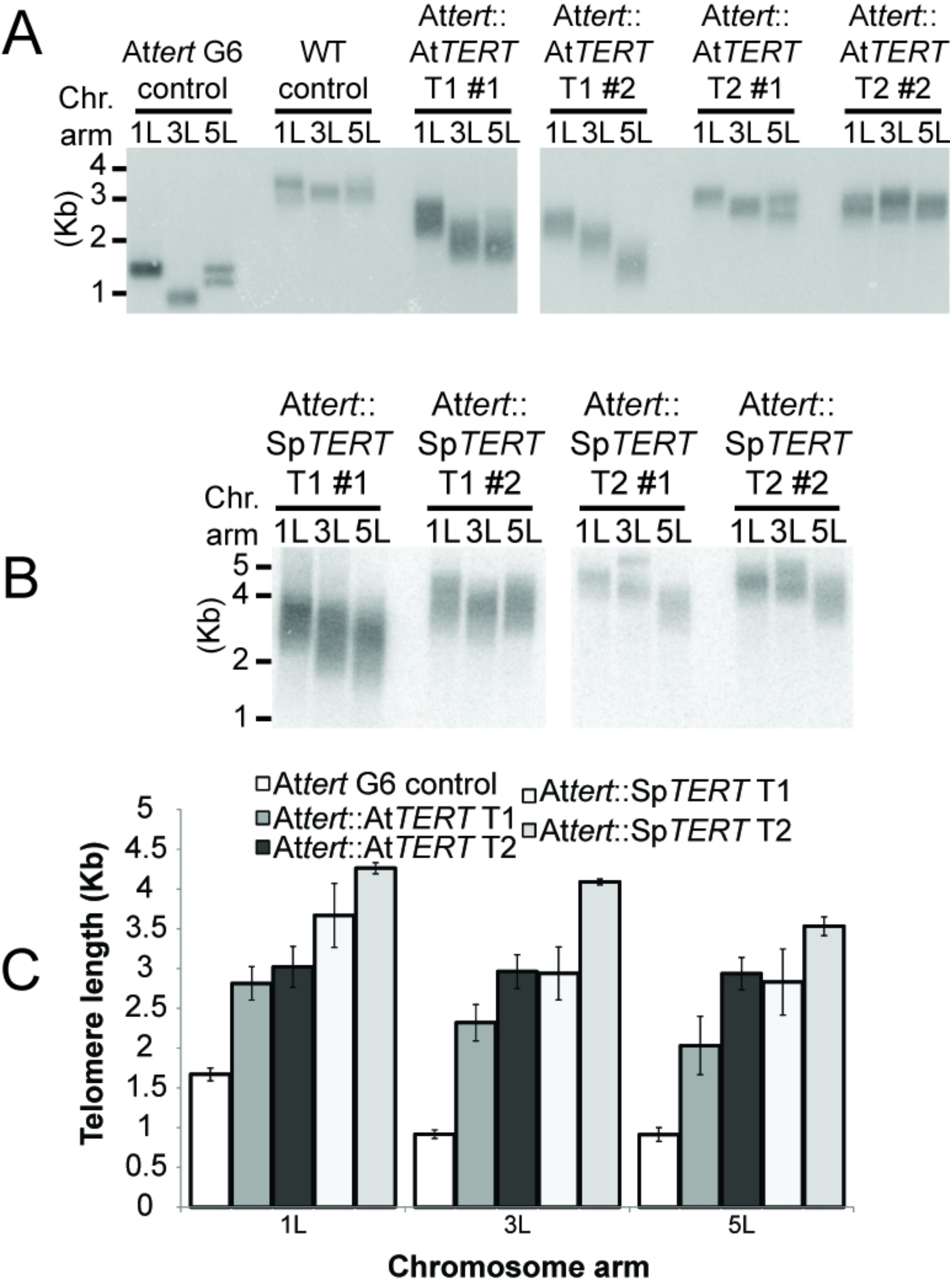
A
Attert G6 control
WT control
Attert:: AtTERT T1 #1
Attert:: AtTERT T1 #2
Attert:: AtTERT T2 #1
Attert:: AtTERT T2 #2
Chr. arm
1L 3L 5L
(Kb)
4
3
2
1
B
Attert:: SpTERT T1 #1
Attert:: SpTERT T1 #2
Attert:: SpTERT T2 #1
Attert:: SpTERT T2 #2
5
4
2
1
C
Attert G6 control
Attert::AtTERT T1
Attert::AtTERT T2
Attert::SpTERT T1
Attert::SpTERT T2
Telomere length (Kb)
5
4.5
4
3.5
3
2.5
2
1.5
1
0.5
0
1L
3L
5L
Chromosome arm

Figure 4

A

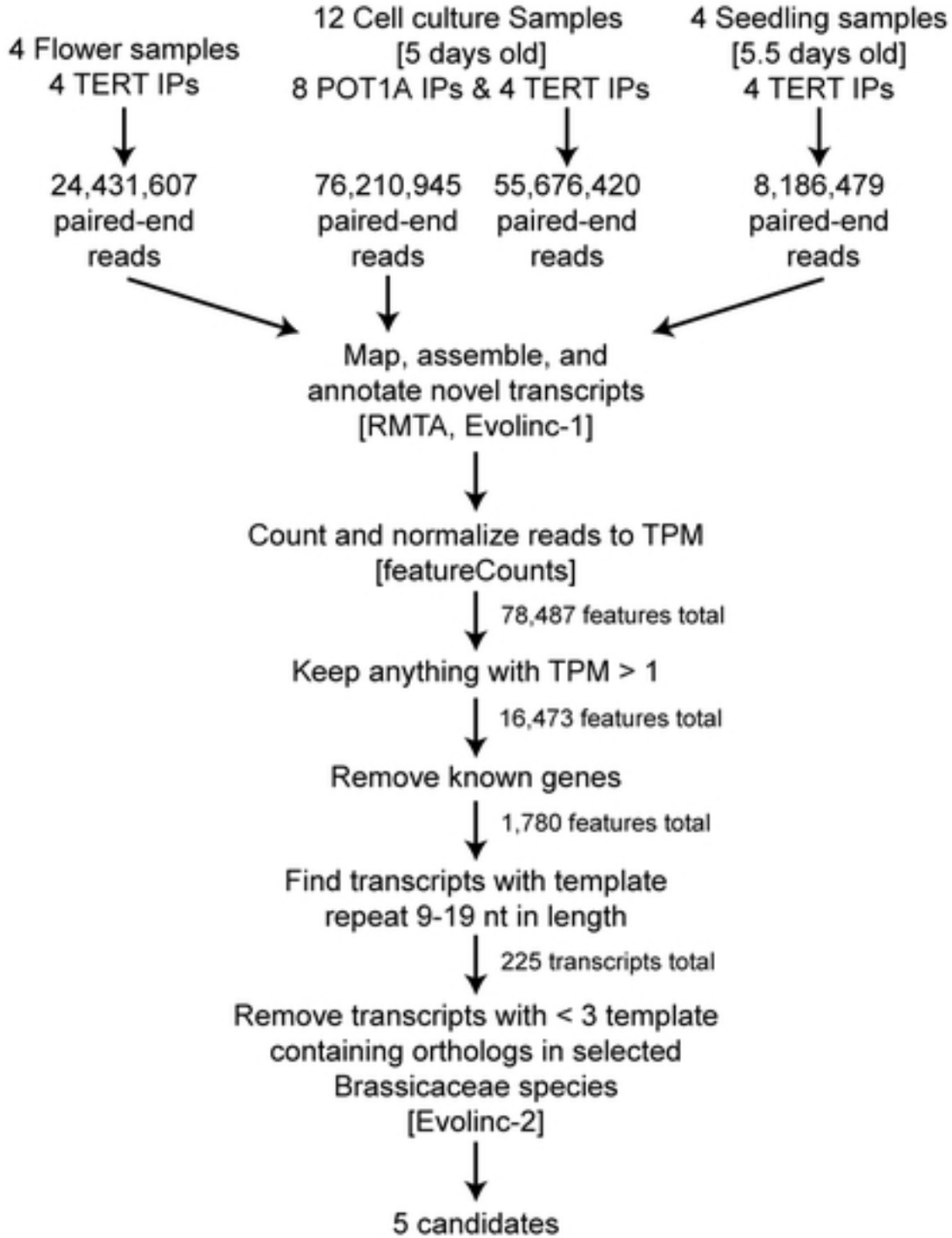

B

Rank	No. of Reads	Average TPM	Locus Length	Template (length)	Chromosome: Position	Longest ORF
#1	4,572	347.05	296 bp	CTAAACCCT 9 nt	2: 12619075-12619370	48 bp
#2	2,276	75.77	846 bp	CCTAAACCCT 10 nt	2: 3496512-3497357	162 bp
#3	389	34.98	242 bp	AAACCCTAAACCC 13 nt	3: 380473-380714	78 bp
#4	349	17.47	541 bp	AAACCCTAA 9 nt	4: 16020834-16021374	141 bp
#5	158	14.80	270 bp	AAACCCTAA 9 nt	2: 8742377-8742646	45 bp

C

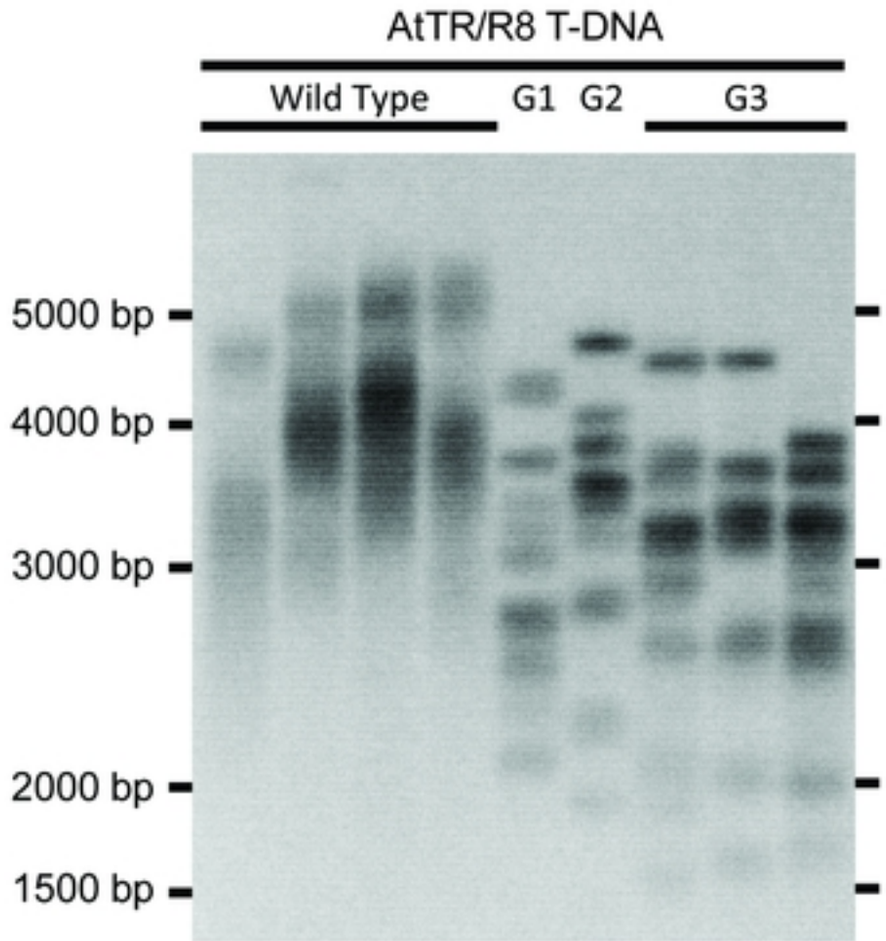

Figure 5

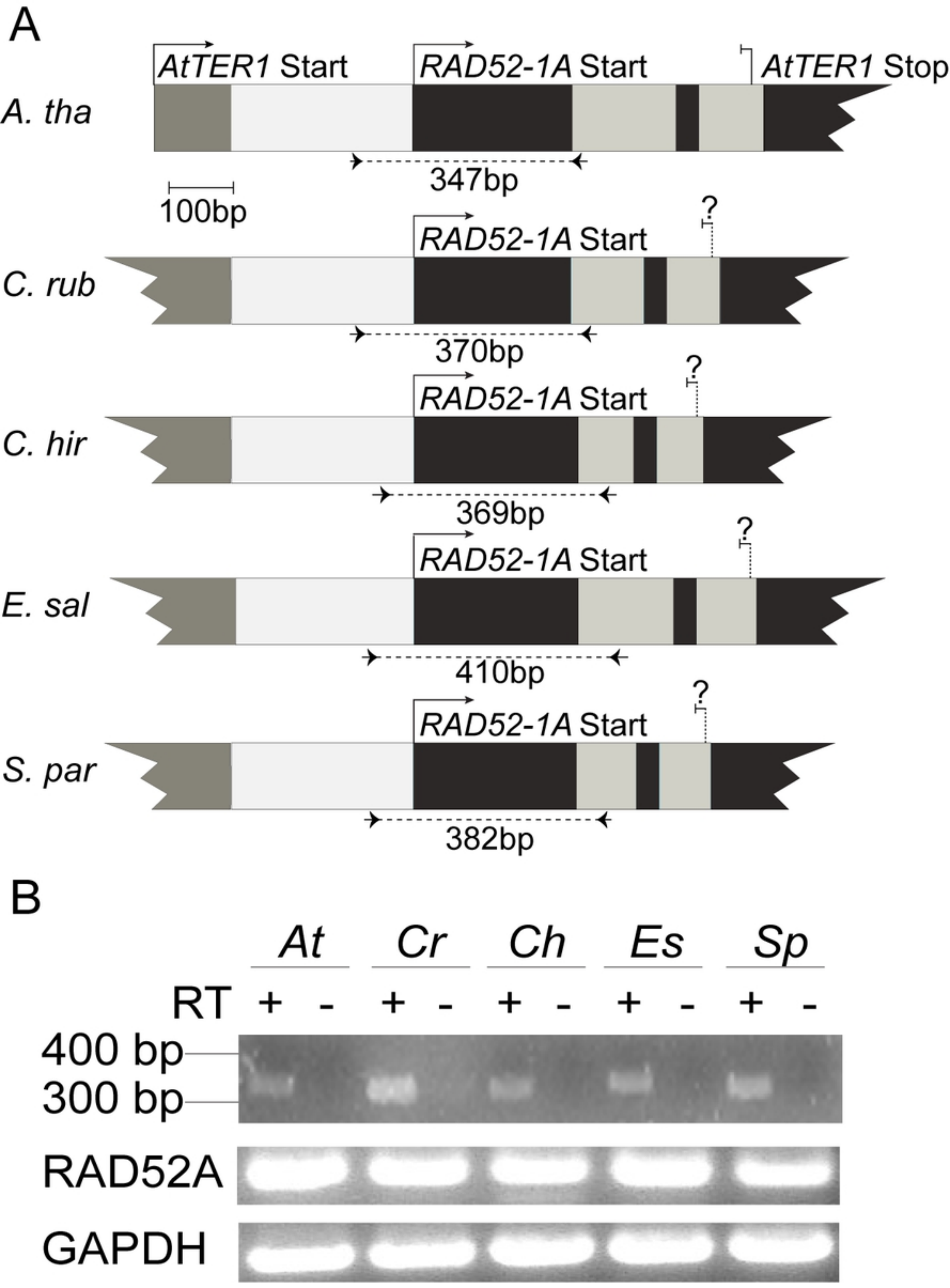
A
AtTER1 Start
RAD52-1A Start
AtTER1 Stop
A. tha
347bp
100bp
RAD52-1A Start
?
C. rub
370bp
RAD52-1A Start
?
C. hir
369bp
RAD52-1A Start
?
E. sal
410bp
RAD52-1A Start
?
S. par
382bp
B
At
Cr
Ch
Es
Sp
RT + - + - + - + - + -
400 bp
300 bp
RAD52A
GAPDH

Figure 6